

A Weighted Gradient Projection Method for Inverse Kinematics of Redundant Manipulators Considering Multiple Performance Criteria

Jun Wan^{1,*} – Jiafeng Yao¹ – Liang'an Zhang² – Hongtao Wu¹

¹ Nanjing University of Aeronautics & Astronautics, College of Mechanical and Electrical Engineering, China

² Anhui University of Technology, Department of Mechanical Engineering, China

Among the many methods of solving inverse kinematics (IK) of redundant manipulators, the classic weighted least-norm (WLN) method is often introduced to avoid joint position limits effectively but cannot be extended to restrict other constraints. Another general technique uses the fashioned gradient projection method (GPM) that ensures successes of the main task and the constraints-based subtasks but suffers with regard to the proper selections for the coefficients of performance criteria. Inspired by the merits of WLN and GPM, a weighted gradient projection method (WGPM) is proposed in this paper to resolve IK problems of redundant manipulators with multiple performance criteria. In this approach, its structure is formulated as a hierarchical task-level regulation, where the highest priority is to accomplish the main task higher than the avoidance of joint position limits, and the priorities of other subtasks of the performance criteria are dependent on the clamping weighted matrix in descending order. Moreover, to avoid the defect of selecting scalar factors for different criteria by trial and error in GPM, a technique of determining proper scalar coefficients is presented by means of normalizing corresponding performance functions in WGPM. Using a 7 degree-of-freedom (DOF) redundant manipulator, simulations and experiments are conducted to demonstrate the validity of the proposed WGPM method by comparing it with the results of the traditional WLN and GPM methods, respectively.

Keywords: inverse kinematics, multiple performance criteria, redundant manipulator, scalar coefficient, weighted gradient projection method

Highlights

- Multiple performance criteria are taken into account in resolving IK problems of redundant manipulators.
- The hierarchical method can guarantee implementations of the main task and the subtasks.
- A scalar coefficient of performance criterion is adjusted on-line by the normalization method.
- The obtained results prove the effectiveness of the proposed WGPM method.

0 INTRODUCTION

Generally, a kinematically redundant manipulator has more DOFs than those required in performing a given task, which can exploit the redundancy to achieve second goals with little influence on the end-effector (EE). At present, the redundant manipulators have attracted considerable interest and been increasingly applied to modern productions and civilian fields.

To solve the inverse kinematics (IK) problem of a robotic manipulator is to obtain a set of actuated joint values to move the manipulator to a desired position and orientation in Cartesian space [1], and is a common basis of dynamic analysis and control system design [2]. Due to the residual redundancy, however, the underdetermined Jacobian matrix of a redundant manipulator admits infinite joint positions corresponding to a given posture of EE. Therefore, the problem of kinematic redundancy resolution becomes the basic and prerequisite issue [3] and [4]. To this end, multiple control strategies have been obtained to the IK resolution as the redundant manipulator has more

degrees-of-freedom (DOFs) over several decades, such as the pseudo-inverse (PI) method, the extended Jacobian matrix (EJM) method, and geometric methods for special structures, apart from the weighted least-norm (WLN) and the gradient projection method (GPM) [5] and [6]. Note that the WLN method and the GPM method are the most frequently used ones, but both methods are seriously flawed. In WLN, the major limitation is that it can only be used to constrain joint position limits effectively and dampen joint motion to exceed the limit without backing away from it. Meanwhile, the scalar factor in GPM for the performance criterion is often selected empirically, which may incur the poor performance of subtasks. Furthermore, a novel solution [7] and [8] to the kinematic analysis of a single-loop reconfigurable 7R (R: revolute joints) mechanism is given based on the algorithm of IK about a general serial 6R manipulator but neglects the advantages of redundancy in the 7R manipulator.

On account of the hierarchical control structure applied by GPM considering multiple constraints-

*Corr. Author's Address: College of Mech. and Electrical Engineering, Nanjing University of Aeronautics & Astronautics, 210016, Nanjing, China, junwanrob@gmail.com

based performance criteria, excellent works have been conducted to avoid or alleviate the difficulty of inaccurate coefficients for performance criteria. A nested GPM [9] and [10] is used to provide fixed scalar weighted value for each performance criterion intuitively. Owing to the lack of adaptability to the changing situations using the fixed weighted values, a redundancy-based approach [11] is presented for GPM to eliminate the negative effect by iteratively solving a system of linear equations. Another way is an improved coefficient matrix [12] to calculate the coefficients of criteria by the magnitudes of the least-norm solution and the homogeneous solution of GPM. Moreover, a motion optimization measure [13] is designed to adjust self-motion coefficients in real time of multiple performance criteria for optimizing redundant robot trajectories using GPM. Additionally, to satisfy joint position limits as a performance criterion effectively, an extended vision of GPM [6] is proposed that refers to the principles of WLN and GPM.

However, the existing techniques still do not perfectly solve the problem of rational coefficients determinations for performance criteria in the original GPM method. They identify these coefficients by using extensive simulations inefficiently and/or increase the computation burden in algorithm unconsciously. Therefore, the self-adjusting coefficients of constraints-based performance criteria are the prerequisite for redundant robot manipulation using the GPM method with high efficiency.

Motivated by the availability of avoiding joint position limits of the WLN method and the extensibility of constraining multiple criteria of the GPM method, a novel GPM method, WGPM, is proposed in this paper to resolve IK problems of redundant manipulators considering multiple performance criteria. Novelties and specific contributions in this work are that in order to eliminate the limitation of the WLN method, a clamping weighted matrix and a repulsive potential field are introduced to force joints back away from joint position limits while not only blocking them at limits. In terms of selecting proper scalar factors for different performance criteria in the proposed weighted gradient projection method (WGPM), a technique of determining continuous scalar coefficients is presented based on respective normalizations of criteria but not on empiricism, which can maintain the performances of subtasks in the WGPM method. In order to regulate the subtasks and avoid conflicts between them, a hierarchy-based resolution on the proposed WGPM method is

presented in which priorities of performance criteria are organized in descending order.

This paper is outlined as follows: Section 1 briefly reviews IK formulations of redundant manipulators, and the WGPM method is proposed in Section 2. To verify and assess the proposed method, results and discussion of simulations and experiments are performed compared to the WLN method and the GPM method, respectively, in Section 3. Finally, the conclusive remarks are shown in Section 4.

1 PROBLEM FORMULATION

In kinematic control, $\dot{\mathbf{x}} \in \mathbf{R}^m$ denotes the main task velocity of a manipulator, and $\dot{\boldsymbol{\theta}} \in \mathbf{R}^n$ denotes the corresponding joint velocities. The relation between them is expressed as follows:

$$\dot{\mathbf{x}} = \mathbf{J}(\boldsymbol{\theta})\dot{\boldsymbol{\theta}}, \quad (1)$$

where $\mathbf{J}(\boldsymbol{\theta}) \in \mathbf{R}^{m \times n}$ is the Jacobian matrix. For redundant manipulators, if $\text{rank}(\mathbf{J})$ keeps constant as m and $m < n$, \mathbf{J} becomes an underdetermined one, and the resolution of Eq. (1) is infinite corresponding to a given task velocity.

By using the PI method, the joint velocity $\dot{\boldsymbol{\theta}}$ can have a least-norm solution

$$\dot{\boldsymbol{\theta}} = \mathbf{J}^+ \dot{\mathbf{x}}, \quad (2)$$

where \mathbf{J}^+ denotes the Moore-Penrose inverse of \mathbf{J} , $\mathbf{J}^+ = \mathbf{J}^T (\mathbf{J}\mathbf{J}^T)^{-1}$. Obviously, the PI method does not exhaust redundancy to perform optimization research for subtasks.

The IK solution, however, cannot always be derived in a straightforward manner as Eq. (2) due to an inherent singularity problem [14]. In order to handle singularities, the IK solution of a redundant manipulator in singular configurations is achieved by utilizing the damped least-squares (DLS) method [15], which has a compromised product between the accuracy of main task motion and the continuities of joint velocities. The DLS method is formally given as:

$$\mathbf{J}^T \dot{\mathbf{x}} = (\mathbf{J}^T \mathbf{J} + \rho^2 \mathbf{I}_n) \dot{\boldsymbol{\theta}}, \quad (3)$$

where $\mathbf{I}_n \in \mathbf{R}^n$ is an identity matrix, and $\rho \geq 0$ is the damping factor. A small value of ρ leads to accurate solutions but low robustness to occurrences of singular and near-singular configurations of the manipulator and vice versa. ρ is usually determined by the following equation:

$$\rho^2 = \max \left\{ 0, \rho_{\max}^2 \left(1 - \left(\frac{\sigma_{\min}}{\varepsilon} \right)^2 \right) \right\} \geq 0, \quad (4)$$

where ρ_{\max} is at the user's disposal to suitably shape the solution in the neighbourhood of a singularity. ε is the size of the singular region. σ_{\min} is the minimum of singularity values from the singular value decomposition (SVD) technique on \mathbf{J} .

Performance criteria play an important role in control that determines the application potential of redundant manipulators [16] and improves kinematics and dynamics performance [17]. Following the consideration, therefore, the motion of the subtask should be appropriately selected based on the criterion with the primary task unaffected, which can be described by GPM:

$$\dot{\boldsymbol{\theta}} = \mathbf{J}^+ \dot{\mathbf{x}} + k \mathbf{P} \nabla \mathbf{H}(\boldsymbol{\theta}). \quad (5)$$

The first item on the right of Eq. (5) is the least-norm solution for the primary task, and the second item is the homogeneous solution for self-motion that is orthogonal to the former in the null space $\mathbf{P} = \mathbf{I}_n - \mathbf{J}^+ \mathbf{J}$. $\nabla \mathbf{H}(\boldsymbol{\theta})$ is the gradient vector of performance criterion $\mathbf{H}(\boldsymbol{\theta})$ as a subtask, which is expressed as:

$$\nabla \mathbf{H}(\boldsymbol{\theta}) = \left[\frac{\partial \mathbf{H}(\boldsymbol{\theta})}{\partial \theta_1}, \frac{\partial \mathbf{H}(\boldsymbol{\theta})}{\partial \theta_2}, \dots, \frac{\partial \mathbf{H}(\boldsymbol{\theta})}{\partial \theta_n} \right]^T. \quad (6)$$

k is the scalar coefficient. It should be taken positive if $\nabla \mathbf{H}(\boldsymbol{\theta})$ is to be maximized, and negative if $\nabla \mathbf{H}(\boldsymbol{\theta})$ is to be minimized. As noted in the previous section, choosing a satisfactory coefficient is non-trivial. If k is too small, the capability for avoiding the constraint is weakened. If k is too large, violating the constraint and causing oscillation during execution is probable.

As an alternative, the WLN method is expressed as follows:

$$\mathbf{J}_w = \mathbf{J} \mathbf{W}^{-\frac{1}{2}}, \quad (7)$$

$$\dot{\boldsymbol{\theta}}_w = \mathbf{W}^{\frac{1}{2}} \dot{\boldsymbol{\theta}}, \quad (8)$$

$$\dot{\boldsymbol{\theta}} = \mathbf{W}^{-\frac{1}{2}} \mathbf{J}_w^+ \dot{\mathbf{x}} = \mathbf{W}^{-1} \mathbf{J}^T (\mathbf{J} \mathbf{W}^{-1} \mathbf{J}^T)^{-1} \dot{\mathbf{x}}, \quad (9)$$

where \mathbf{J}_w and $\dot{\boldsymbol{\theta}}_w$ are defined as the weighted Jacobian matrix and the weighted joint velocity, respectively. $\mathbf{W} \in \mathbf{R}^{n \times n}$ is the positive and diagonal weighted matrix, and its i^{th} diagonal element is defined by:

$$w_i = \begin{cases} 1 + \left| \frac{\partial \mathbf{H}(\boldsymbol{\theta})}{\partial \theta_i} \right| & \Delta \left| \frac{\partial \mathbf{H}(\boldsymbol{\theta})}{\partial \theta_i} \right| \geq 0 \\ 1 & \text{else} \end{cases}, \quad (10)$$

where $\Delta \left| \frac{\partial \mathbf{H}(\boldsymbol{\theta})}{\partial \theta_i} \right|$ is the change rate of $\left| \frac{\partial \mathbf{H}(\boldsymbol{\theta})}{\partial \theta_i} \right|$ [18].

The WLN method is proposed to only keep joint motion inside a physical range based on a performance criterion:

$$\mathbf{H}(\boldsymbol{\theta}) = \sum_{i=1}^n \frac{(\theta_{\max} - \theta_{\min})^2}{4(\theta_{\max} - \theta_i)(\theta_i - \theta_{\min})}, \quad (11)$$

where θ_{\max} and θ_{\min} are the upper and lower limits of the joint position θ_i .

In Fig. 1, when θ_i is gradually close to the neighbouring positive or negative limit, $\left| \frac{\partial \mathbf{H}(\boldsymbol{\theta})}{\partial \theta_i} \right| \rightarrow \infty$, this is, $w_i \rightarrow \infty$. Therefore from Eq. (9), $\dot{\theta}_i$ is repressed to zero, and the i^{th} joint motion is stopped at limit and has no competence to withdraw the joint from its limit.

Both GPM and WLN are possible to risk singularities when the manipulator configuration is ill-conditioned. Combining the DLS method defined in Eq. (3), GPM could be rewritten as:

$$\dot{\boldsymbol{\theta}} = \mathbf{J}_a^+ \dot{\mathbf{x}} + k(\mathbf{I}_n - \mathbf{J}_a^+ \mathbf{J}) \nabla \mathbf{H}(\boldsymbol{\theta}), \quad (12)$$

$$\mathbf{J}_a^+ = \mathbf{J}^T (\mathbf{J} \mathbf{J}^T + \rho^2 \mathbf{I}_m)^{-1}. \quad (13)$$

WLN could be redefined by:

$$\dot{\boldsymbol{\theta}} = \mathbf{W}^{-1} \mathbf{J}^T (\mathbf{J} \mathbf{W}^{-1} \mathbf{J}^T + \rho^2 \mathbf{I}_m)^{-1} \dot{\mathbf{x}}, \quad (14)$$

where $\mathbf{I}_m \in \mathbf{R}^m$ is an identity matrix.

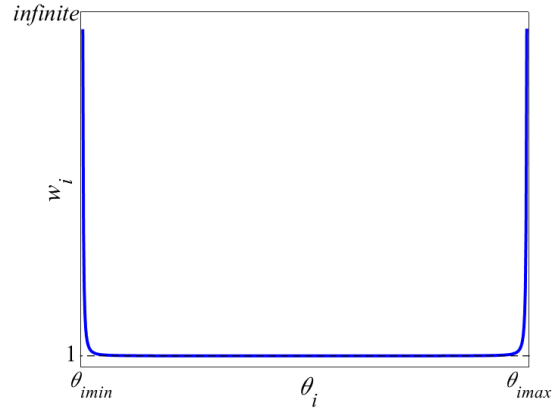


Fig. 1. Weighted value for the i^{th} joint position in WLN

2 FORMULATION OF WGPM

2.1 Progressive Clamping Weighted Matrix

We add an activation buffer, i.e., a band of width Ω , before a joint position limit, so that a whole joint motion interval is divided into three parts, as depicted in Fig. 2.

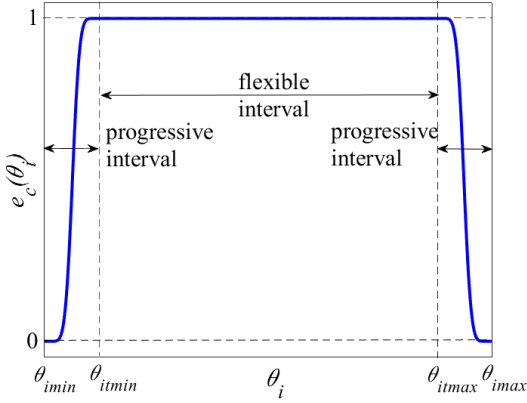


Fig. 2. Weighted value for the i^{th} joint position in WGPM

Hence, a progressive clamping weighted matrix is defined by:

$$\mathbf{E}_c = \text{diag}(e_c(\theta_i)), \quad i = 1, 2, \dots, n, \quad (15)$$

where the element $e_c(\theta_i)$ is governed by:

$$e_c(\theta_i) = \begin{cases} g_\Omega\left(\frac{\theta_{itmin} - \theta_i}{\theta_{itmin} - \theta_{imin}}\right) & \theta_{imin} \leq \theta_i \leq \theta_{itmin} \\ 1 & \theta_{itmin} < \theta_i < \theta_{itmax} \\ g_\Omega\left(\frac{\theta_i - \theta_{itmax}}{\theta_{imax} - \theta_{itmax}}\right) & \theta_{itmax} \leq \theta_i \leq \theta_{imax} \end{cases}, \quad (16)$$

where θ_{itmax} , θ_{itmin} are the upper and lower damping thresholds before θ_{imax} and θ_{imin} , respectively, and $\theta_{itmax} = (1-\Omega)\theta_{imax} + \Omega\theta_{imin}$, $\theta_{itmin} = (1-\Omega)\theta_{imin} + \Omega\theta_{imax}$. $g_\Omega(\bullet)$ is a transitional function for the weighted factor varying from one to zero:

$$g_\Omega(d) = \frac{1}{2} - \frac{1}{2} \tanh\left(\frac{1}{1-d} - \frac{1}{d}\right), \quad d \in [0, 1]. \quad (17)$$

Based on the control technique in Eq. (16), an activation buffer is successfully taken into consideration that ensures the continuity and boundedness of the clamping weighted factor. In other words, when the joint motion runs in the flexible interval, the weighted value remains constant as one. While the joint goes towards the progressive interval from the flexible interval, the technique enables the weighted value to decrease uninterruptedly from one until zero, restricted at the joint position limit. Therefore, the continuous clamping weighted factor defined in Eq. (16) discards any unnecessary change of weighted value in the flexible region, in comparison to Eq. (10).

2.2 Repulsive Potential Field

Similar to the framework of WLN, the clamping control in this paper is designed

$$\dot{\theta} = \mathbf{E}_c \mathbf{J}_{E_c}^\oplus \dot{\mathbf{x}}, \quad (18)$$

where $\mathbf{J}_{E_c} = \mathbf{J} \mathbf{E}_c$ is a weighted Jacobian matrix based on \mathbf{E}_c and $\mathbf{J}_{E_c}^\oplus = \mathbf{E}_c \mathbf{J}^T (\mathbf{J} \mathbf{E}_c \mathbf{J}^T)^{-1}$.

When $\mathbf{E}_c = \mathbf{I}_n$, Eq. (18) is equal to Eq. (2). While $e_c(\theta_i) \rightarrow 0$, we find it does not push θ_i from the position limit but blocks any motion beyond the limit. However, referring to the potential field methods applied to avoid obstacles in IK resolutions of redundant manipulators [19], we define a repulsive task $\mathbf{J}_{B_k} \mathbf{T}_r$ to force θ_i back far from its limit that is depended on the joint positions and orthogonal to the primary task by means of being projected onto the weighted null space $\mathbf{P}_{E_c}^\oplus$. Therefore, a novel control scheme is represented as:

$$\theta = \mathbf{E}_c \mathbf{J}_{E_c}^\oplus \dot{\mathbf{x}} - \mathbf{P}_{E_c}^\oplus \mathbf{J}_{B_k} \mathbf{T}_r, \quad (19)$$

where $\mathbf{P}_{E_c}^\oplus = \mathbf{I}_n - \mathbf{J}_{E_c}^\oplus \mathbf{J}_{E_c}$, $\mathbf{J}_{B_k} = \mathbf{I}_n - \mathbf{E}_c$ indicates the weighted constraint Jacobian matrix for the repulsive task. $\mathbf{T}_r = \text{diag}(t_r(\theta_i))$ is the repulsive force, whose element $t_r(\theta_i)$ is designed by:

$$t_r(\theta_i) = \begin{cases} \frac{\theta_i - \theta_{itmin}}{\theta_{itmin} - \theta_{imin}} t_{rmax} & \theta_{imin} \leq \theta_i \leq \theta_{itmin} \\ 0 & \theta_{itmin} < \theta_i < \theta_{itmax} \\ \frac{\theta_i - \theta_{itmax}}{\theta_{imax} - \theta_{itmax}} t_{rmax} & \theta_{itmax} \leq \theta_i \leq \theta_{imax} \end{cases}, \quad (20)$$

t_{rmax} denotes the maximum potential field force. The closer to the limit it is, the stronger the repulsive potential force is.

When joints are all located within the flexible interval, $\mathbf{J}_{B_k} = \mathbf{0}$, Eq. (19) acts as Eq. (2). While a joint remains in the progressive interval, $\mathbf{J}_{B_k} \neq \mathbf{0}$, the clamping and repulsive potential force are activated and withdraw the joint motion away from limit as far as possible. While the joint θ_i reaches its limit, $e_c(\theta_i) \rightarrow 0$, the clamping term is disabled but $t_r(\theta_i)$ becomes greatest and to push the joint motion away from its limit plays a dominant role in controlling. However, since $\mathbf{P}_{E_c}^\oplus \mathbf{J}_{B_k} \mathbf{T}_r$ is a homogeneous solution, therefore, the main task of the manipulator is not affected.

Note that the manipulator could degenerate when it enters the singular region. According to the DLS method, Eq. (19) is arranged in the form:

$$\dot{\theta} = \mathbf{E}_c \mathbf{J}_{E_c}^{\oplus, P_{E_c}} \dot{\mathbf{x}} - \mathbf{P}_{E_c}^{\oplus, P_{E_c}} \mathbf{J}_{B_k} \mathbf{T}_r, \quad (21)$$

where $\mathbf{J}_{E_c}^{\oplus, \rho_{E_c}}$, $\mathbf{P}_{E_c}^{\oplus, \rho_{E_c}}$ are reproduced from $\mathbf{J}_{E_c}^{\oplus}$ and $\mathbf{P}_{E_c}^{\oplus}$ based on the DLS method. The damping factor ρ_{E_c} is derived from Eq. (4) by substituting \mathbf{J}_{E_c} for \mathbf{J} .

2.3 Continuous Scalar Coefficient

Eq. (21) is defined to improve the redundant manipulator performance of avoiding joint position limits. However, when the manipulator is executing tasks under the complicated conditions of multiple constraints, Eq. (21), thus, cannot generate feasible joint velocity. Therefore, pertinent performance criteria for the joint motion have to be considered.

To solve such a problem generally requires compiling multiple criteria as a sum over weighted subtasks' quadratic functions, and a trade-off of the main task and subtasks is performed by the manual tuning of the weights [20], which is often expressed as:

$$\phi = \sum_{j=1}^s k_j \nabla \mathbf{H}_j, \quad (22)$$

where k_j is the fixed scalar factor for the j^{th} performance criterion H_j , and is selected empirically. s indicates the total number of performance criteria.

However, the units and magnitudes of multiple criteria may differ from each other so that the assignation of k_j for each criterion through experience can allow critical limitations in terms of balancing the strengths of the criteria in control. Therefore, normalization is required to obtain the same magnitude of each criterion for assigning an appropriate scalar factor. Since the fixed scalar factors are not applicable to any configurations of the manipulator, in this paper, the continuous scalar factor $k_j(H_{nj})$ is redefined based on its normalization:

$$k_j(H_{nj}) = \pm f(H_{nj}), \quad (23)$$

where $\pm f(\bullet)$ denotes a continuous function, and its sign is selected positively if the performance criterion is to be maximized and vice versa. H_{nj} is the normalized value of the criterion H_j .

For avoiding unnecessary optimizations of criteria when the configuration of the manipulator is in its most balanced state, hence, analogous to Eq. (16), the maximum and minimum normalized thresholds, $H_{nj}^{M_t}$ and $H_{nj}^{m_t}$, are defined as:

$$H_{nj}^{M_t} = (1 - \lambda)H_{nj}^M + \lambda H_{nj}^m, \quad (24)$$

$$H_{nj}^{m_t} = (1 - \lambda)H_{nj}^m + \lambda H_{nj}^M, \quad (25)$$

where H_{nj}^M and H_{nj}^m indicate the upper and lower boundaries of H_{nj} , respectively. λ controls the bandwidth between $H_{nj}^{M_t}$ ($H_{nj}^{m_t}$) and H_{nj}^M (H_{nj}^m).

To obtain a continuous scalar factor, the continuous function $f(\bullet)$ is expressed as follows:

$$f(H_{nj}) = \begin{cases} 1 & H_{nj}^m \leq H_{nj} \leq H_{nj}^{M_t} \\ aH_{nj}^3 + bH_{nj}^2 + cH_{nj} + d & H_{nj}^{M_t} < H_{nj} < H_{nj}^M \\ 0 & H_{nj}^{M_t} \leq H_{nj} \leq H_{nj}^M \end{cases}, \quad (26)$$

where

$$a = -\frac{2}{(H_{nj}^{m_t})^3 - 3(H_{nj}^{m_t})^2 H_{nj}^{M_t} + 3H_{nj}^{M_t}(H_{nj}^{M_t})^2 - (H_{nj}^{M_t})^3},$$

$$b = \frac{3H_{nj}^{m_t} + 3H_{nj}^{M_t}}{(H_{nj}^{m_t})^3 - 3(H_{nj}^{m_t})^2 H_{nj}^{M_t} + 3H_{nj}^{M_t}(H_{nj}^{M_t})^2 - (H_{nj}^{M_t})^3},$$

$$c = -\frac{6H_{nj}^{m_t} H_{nj}^{M_t}}{(H_{nj}^{m_t})^3 - 3(H_{nj}^{m_t})^2 H_{nj}^{M_t} + 3H_{nj}^{M_t}(H_{nj}^{M_t})^2 - (H_{nj}^{M_t})^3},$$

$$d = \frac{3H_{nj}^{m_t}(H_{nj}^{M_t})^2 - (H_{nj}^{M_t})^3}{(H_{nj}^{m_t})^3 - 3(H_{nj}^{m_t})^2 H_{nj}^{M_t} + 3H_{nj}^{M_t}(H_{nj}^{M_t})^2 - (H_{nj}^{M_t})^3}.$$

In Fig. 3, it is obvious that the curve is monotonously decreasing and continuous. When $k_j \rightarrow 1$, the influence of the j^{th} performance criterion becomes increasingly evident in the resolution of IK for the redundant manipulator. Conversely, when $k_j \rightarrow 0$, the criterion is increasingly deprived of the IK resolution.

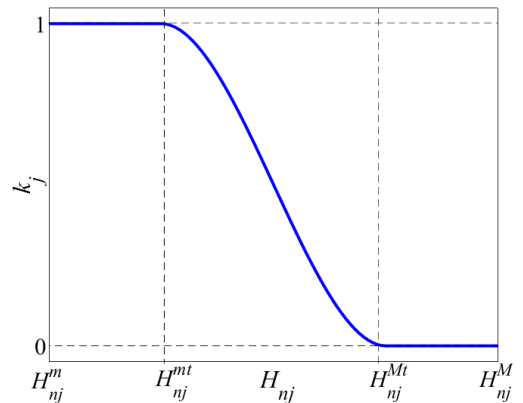


Fig. 3. A scalar coefficient for the corresponding performance criterion by calculation

2.4 Normalizing Criteria

Before normalization, the type and optimal value distribution of the performance criterion should be considered and analysed. For simplicity, assume a

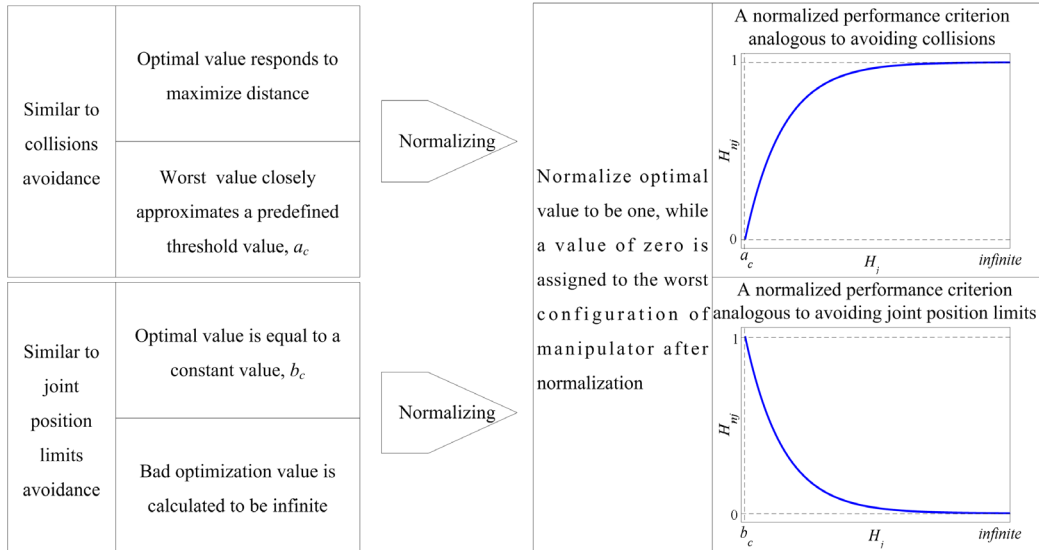


Fig. 4. A principle utilized to normalize different performance criteria

performance criterion is optimized by maximization or minimization in this paper.

For instance, in the case of avoiding collisions, the distance between EE and an obstacle is often defined as a performance criterion, which is supposed to maximize the distance but to oppose a small one, especially tending to the distance of zero.

Taking the avoidance of joint position limits defined as Eq. (11) as another example, the optimal value for each joint is equal to one as the joint position is in the middle of its limit, while the value becomes infinite when the joint goes towards the limit. Thus, the distribution of optimal value of avoiding joint position limits is the opposite of the case of avoiding collisions.

Consequently, distributions of optimal values vary from different performance criteria. For normalizing these individuals, we assume normalization for a criterion conforms to the following principle illustrated in Fig. 4.

To normalize the criteria similar to collisions avoidance, an exponential function is defined to normalize this kind of criteria

$$N_{\infty}(H_j) = 1 - \exp(a_c - H_j), \quad (27)$$

where $N_{\infty}(\infty)=1$ denotes the optimal normalized value far away from the predefined threshold a_c , and $N_{\infty}(a_c)=0$ indicates the manipulator is in the configurations that are restrained strictly.

On contrary, to normalize the criteria analogous to avoidance of the joint position limits where the

optimal value tends to a constant value b_c rather than infinite, we define another an exponential function for normalizations of these performance criteria

$$N_c(H_j) = \exp(b_c - H_j), \quad (28)$$

where $N_c(b_c)=1$ shows the optimal configuration of the manipulator without poor performances, e.g., $H_j=\infty$ far greater than b_c , correspondingly, $N_c(\infty)=0$.

Based on the principles defined in Fig. 4, the same closed-range of normalized results can be obtained with the optimum to be one and the inferior to be zero, despite different properties of different performance criteria.

2.5 Resolution of WGPM

Therefore, we can obtain a novel GPM method, WGPM, considering multiple criteria, which is presented as:

$$\dot{\theta} = E_c J_{E_c}^{\oplus, P_{E_c}} \dot{x} - P_{E_c}^{\oplus, P_{E_c}} (J_{B_k} T_r + \sum_{j=1}^s k_j(H_{\eta_j}) \nabla H_j). \quad (29)$$

In complicated circumstances, the criteria may be numerous, and their priority may be varied [20]. Specifically, if some performance criteria are activated simultaneously, criteria exhibit irregularities that affect the redundancy resolution of the manipulator. To regulate multiple criteria and improve the stability of the WGPM method, we set different priorities for criteria through weighted null space. Thus, Eq. (29) is rewritten as a hierarchy-based resolution:

$$\dot{\theta} = E_c J_{E_c}^{\oplus, \rho_{E_c}} \dot{x} - P_{E_c}^{\oplus, \rho_{E_c}} \times (J_{B_k} T_r + \sum_{j=1}^s k_j (H_{nj}) \exp(\frac{1-j}{s} E_c) \nabla H_j), \quad (30)$$

where the defined clamping weighted matrix E_c dominates other criteria, and priorities decrease as the number of subtasks increases.

When $E_c = I_n$, the repulsive potential field is inactive, but other performance criteria are active. However, when $E_c \neq I_n$, the repulsive potential field is activated to repel joints from their position limits, and the impacts of other performance criteria are reduced but not eliminated. Therefore, besides the main task, the priority of avoiding joint position limits is higher than any other criteria in the proposed hierarchical task-level regulation. As the joint motion reaches the singular region ε , the manipulator has to encounter a singularity, $\rho_{E_c} > 0$. Then Eq. (30) is nothing but the solution of the following damped least-squares problem:

$$\min_{\theta} (\|\dot{x} - J\dot{\theta}\|^2 + \rho_{E_c}^2 \|E_c^{-1} \dot{\theta}\|^2). \quad (31)$$

Obviously, Eq. (30) is a compromise product between the feasibility of joint velocities and deviations of main tasks. That is to say, when $E_c \rightarrow 0$, the least-norm solution in Eq. (30), $E_c J_{E_c}^{\oplus, \rho_{E_c}} \dot{x} \rightarrow 0$, and the homogeneous solution

$$-P_{E_c}^{\oplus, \rho_{E_c}} (J_{B_k} T_r + \sum_{j=1}^s k_j (H_{nj}) \exp(\frac{1-j}{s} E_c) \nabla H_j) \rightarrow -P_{E_c}^{\oplus, \rho_{E_c}} J_{B_k} T_r$$

can no longer take effect in the weighted null space $P_{E_c}^{\oplus, \rho_{E_c}}$ due to the existence of ρ_{E_c} and change the task priority to make optimization of avoiding joint position limits have higher priority than the main task motion.

3 RESULTS AND DISCUSSION

Simulations and experiments are constructed to demonstrate the effectiveness and practicability of the proposed WGPM method for IK resolutions of redundant manipulators. In this work, a 7-DOF redundant manipulator is taken as an analysis object, shown in Fig. 5. The D-H parameters of the manipulator with the allowable limits for joint positions and joint velocities are listed in Table 1, where $m_2 = -0.2975$, $m_3 = -0.3555$, $l_1 = 0.45$, $m_4 = -0.293$, $l_2 = 0.4$, $m_5 = 0.255$, $m_6 = 0.197$, $m_7 = 0.104$.

To improve motion precision, the closed-loop algorithm is introduced that is expressed as:

$$\dot{x} = \dot{x}_d + \kappa E_e, \quad (32)$$

where \dot{x}_d is the desired trajectory. κ is the positive feedback gain, and is set to 80. $E_e \in R^{6 \times 1}$ indicates the tracking error between the desired and actual trajectory

$$E_e = \begin{bmatrix} P_d - P \\ 0.5(n \times n_d + s \times s_d + a \times a_d) \end{bmatrix}, \quad (33)$$

$P_d \in R^{3 \times 1}$, $P \in R^{3 \times 1}$ are the vectors of the desired and actual position of EE, and $R_d = (n_d, s_d, a_d) \in R^{3 \times 3}$, $R = (n, s, a) \in R^{3 \times 3}$, express the rotation matrices for the desired and actual orientations of EE, respectively.

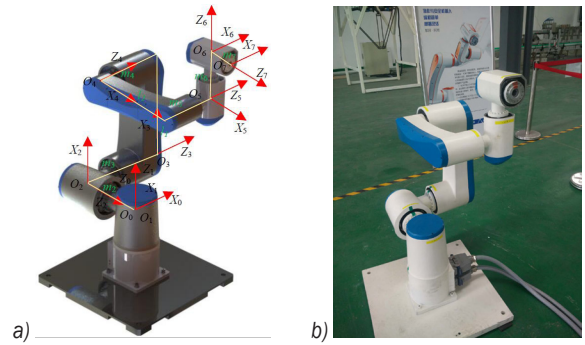


Fig. 5. A 7-DOF redundant manipulator; a) kinematic model, b) physical prototype

Table 1. D-H parameters and joint limits

i	α_{i-1} [°]	a_{i-1} [m]	d_i [m]	θ_i [°]	$\theta_{imin} \sim \theta_{imax}$ [°]	v_{imax} [°/s]
1	0	0	0	q1	-160 ~ 160	55
2	90	0	m_2	q2	-33 ~ 150	55
3	90	0	m_3	q3	-165 ~ 80	55
4	0	l_1	m_4	q4	-180 ~ 40	55
5	0	l_2	m_5	q5	-150 ~ 150	65
6	90	0	m_6	q6	-180 ~ 180	65
7	90	0	m_7	q7	-180 ~ 180	65

Furthermore, the simulations in the paper are implemented with the aid of the Matlab R2016a tool, and in the experiment, a computer with Intel Core i3 @ 1.8 GHz processor & 2 GB RAM as the control platform and the LabVIEW 2016 as the operation software are utilized to control servo joints connected in the manipulator with a sampling time of 0.005 s.

3.1 Numerical Simulations of Clamping and Repulsive Force

As a validation of the proposed clamping and repulsive potential field, we only consider the avoidance of joint position limits as a subtask in redundancy resolution

of the manipulator. Therefore, scalar factors in Eq. (30) for other criteria are set to zero manually. For comparisons, the WLN method defined in Eq. (14) is provided as well.

WLN:

$$\dot{\theta} = W^{-1} J^T (JWJ^T + \rho^2 I_6)^{-1} (\dot{x}_d + \kappa E_e), \quad (34)$$

WGPM:

$$\dot{\theta} = E_c J_{E_c}^{\oplus, \rho_{E_c}} (\dot{x}_d + \kappa E_e) - J_{E_c}^{\oplus, \rho_{E_c}} J_{B_k} T_r, \quad (35)$$

where ρ and ρ_{E_c} are damping factors of WLN and WGPM reduced from Eq. (4) where $\varepsilon=0.02$, $\rho_{\max}=0.02$, and σ_{\min} are the minimum singular values of J_w and J_{E_c} , respectively.

In simulations, we control the manipulator to track a straight-line path whose position is interpolated with the modified trapezoidal function and orientation expressed as Euler angles is planned with the five-order polynomial function. The initial posture of EE is

$$P_s = [0.3174, -0.2065, 0.6469] \text{ [m]},$$

$$O_s = [-90, 90, 90] \text{ [degree]},$$

and terminal posture is

$$P_f = [0.37, 0.0068, 0.1707] \text{ [m]}$$

$$O_f = [-1.0036, 94.9841, -116.8194] \text{ [degree]}.$$

It is noted that the specified path is beyond the reachability of the redundant manipulator, and the fourth joint position in the terminal posture is close to its limit deliberately.

Simulation results of the WLN method are shown in Fig. 6. It is found that WLN comes to suffer from singularity at $t=0.14$ s in Fig. 6c.

However, with the assistance of the DLS method, the continuity of joint velocity in Fig. 6b is still ensured at the expense of deviation of tracking trajectory, i.e., the WLN method obtains the maximum position error at $t=0.28$ s in Fig. 6d. Fig. 6a depicts the normalized joint position expressed as $(2\theta_i - \theta_{i\max} - \theta_{i\min}) / (\theta_{i\max} - \theta_{i\min})$. Obviously, the fourth joint position is damped at limit due to the effect of the penalty function defined in Eq. (11), yielding an increasing weighted factor for the fourth joint shown in Fig. 6e.

Fig. 7 illustrates the simulation results of the proposed WGPM method. To force joints back away from their position limits effectively, the width of the progressive buffer, Ω , is set to 0.25, and the maximum potential field force, $t_{r\max}$, is equal to π . From Fig. 7d, singularity resulted from WGPM occurs later than that from WLN, and as observed in Fig. 7a, the fourth joint position is restrained into the specified range but not violate the limit compared to that in WLN. The fundamental cause for this lies in the action of the repulsive potential field $J_{B_k} T_r$ in the WGPM control where a large velocity is obtained based on the clamping weighted factors in Fig. 7f and projected onto the weighted null space $P_{E_c}^{\oplus, \rho_{E_c}}$ with opposite direction, as shown in Fig. 7c, exploited to push the fourth joint away from the limit. Meanwhile, the seventh joint is effectively kept away from its position limit in comparison with that in the WLN method.

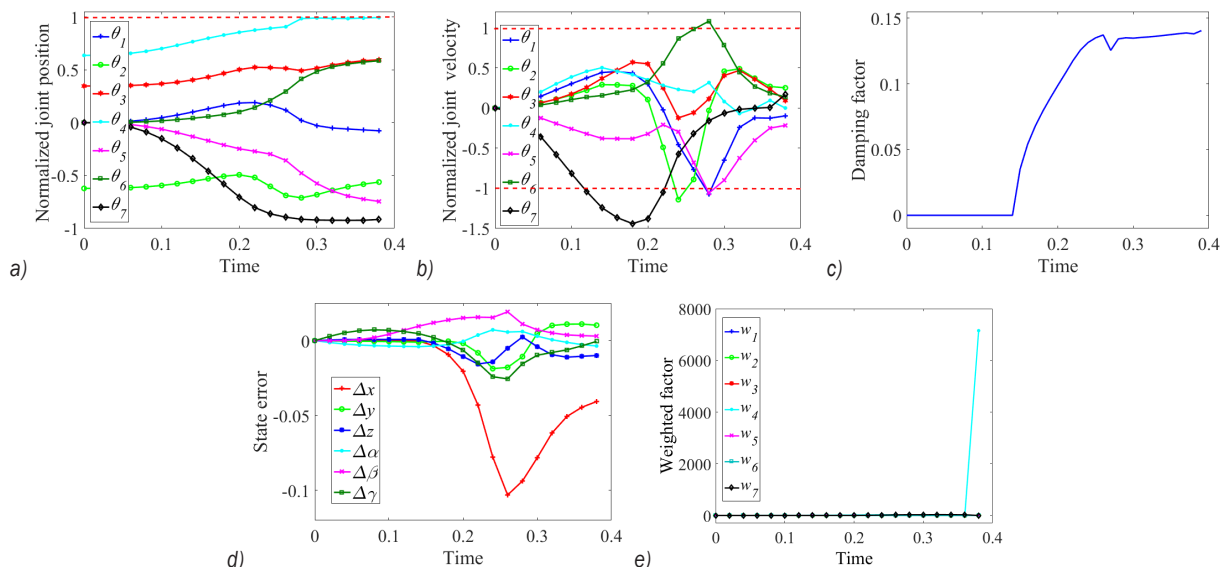


Fig. 6. Simulation results of the WLN method; a) normalized joint position, b) normalized joint velocity, c) damping factor, d) state error including position errors and orientation errors, and e) weighted factor

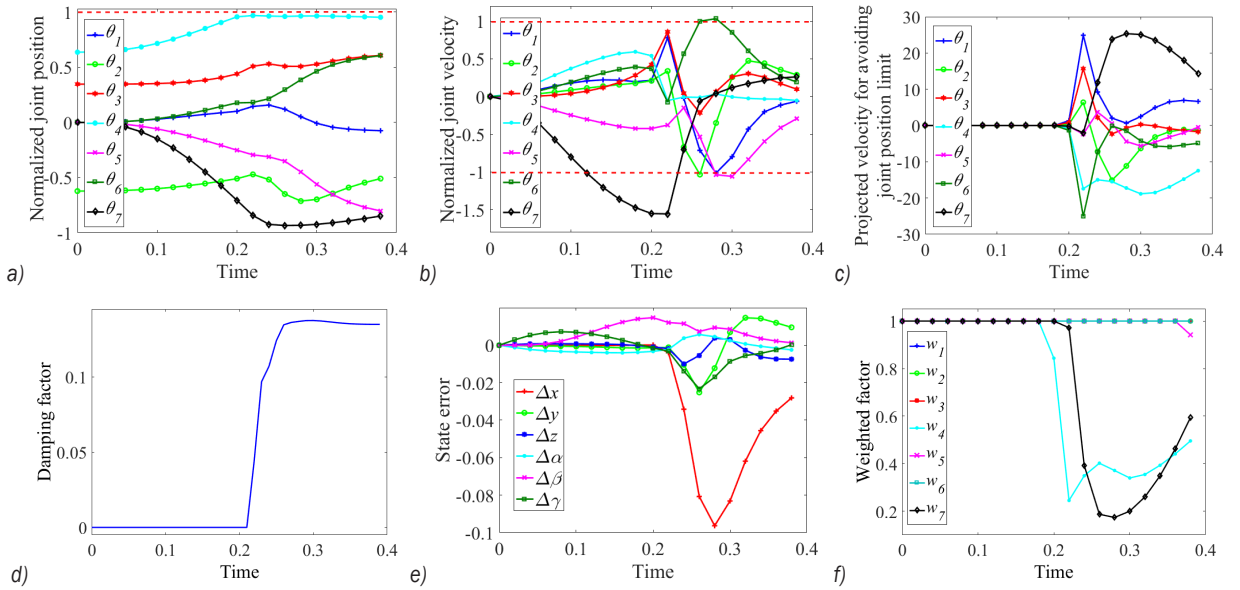


Fig. 7. Simulation results of the proposed WGPM method; a) normalized joint position, b) normalized joint velocity, c) projected velocity produced from the repulsive potential field, d) damping factor, e) state error including position errors and orientation errors, and f) weighted factor composing the clamping matrix

Table 2. The maximum simulation results of state errors

	WLN	WGPM	Percentage [%]
Max Δx [m]	-0.1031	-0.0963	6.6
Max Δy [m]	-0.0209	-0.0212	-1.44
Max Δz [m]	-0.0162	-0.01	38.27
Max $\Delta \alpha$ [rad]	0.0072	0.0057	20.83
Max $\Delta \beta$ [rad]	0.0192	0.0147	23.44
Max $\Delta \gamma$ [rad]	-0.0256	-0.0233	8.98
Running time [s]	0.2337	0.1832	21.61

Table 2 briefly shows the maximum simulation results of state errors generated from WLN and WGPM. It is found that except along the direction of the Y -axis, the proposed WGPM method significantly increases the motion accuracy compared to the WLN method, which reduces position errors by 6.6 %, 38.27 % along the X and Z axes, and orientation errors by 20.83 %, 23.44 %, and 8.98 %. Meanwhile, since the WGPM method only performs optimizations when the joint position steps into the defined progressive interval while the WLN method optimizes the joint position throughout the whole interval, WGPM avoids the unneeded optimization procedure and improves the computational efficiency by 21.61 %.

Consequently, the simulation results indicate that the efficiency of the proposed WGPM method with clamping weighted matrix and repulsive potential field is superior to the traditional WLN method.

However, from Figs. 6b and 7b, except the third joint and the fourth joint, other joint velocities exceed their limits shown as normalizations, which is not admitted to appear in the physical control of manipulator. Thus, the problem will be resolved in the following experiment and the performance of the proposed WGPM method with multiple criteria will be verified.

3.2 Experimental Verification with Multiple Criteria

As the joint velocity violates its limit in the above simulations, joint velocity commands may lose effect when large instantaneous task velocity is requested, causing significant velocity saturations [21]. Analogous to the criterion of avoiding joint position limits expressed as Eq. (11), the performance criterion of avoiding joint velocity limits is defined as:

$$G(\dot{\theta}_i) = \sum_{i=1}^7 \frac{(\dot{\theta}_{i\max} - \dot{\theta}_{i\min})^2}{4(\dot{\theta}_{i\max} - \dot{\theta}_i)(\dot{\theta}_i - \dot{\theta}_{i\min})}, \quad (36)$$

where $\dot{\theta}_{i\max}$ (expressed as $v_{i\max}$ in Table 1), $\dot{\theta}_{i\min} = -\dot{\theta}_{i\max}$ are the maximum and minimum of the i th joint velocity, respectively. This also complies with the principle of normalizing a performance criterion defined in Fig. 4.

The experiment focuses on the realization of the main tasks under the joint limit constraints such as joint position limits and joint velocity limits. The comparison with the conventional GPM method is

devised to validate the superiority of the proposed WGPM method in this case. Therefore, combining Eqs. (11), (12) and (36), the conventional GPM method with fixed scalar factors for multiple criteria is written as:

$$\dot{\theta} = J_a^+(\dot{x}_d + \kappa E_e) + (I_7 - J_a^+ J)(k_H \nabla H(\theta) + k_G \nabla G(\dot{\theta})), \quad (37)$$

where k_H , k_G are the fixed scalar coefficients to regulate the projected velocities of avoiding joint position limits and joint velocity limits and are set to -0.1 and -0.05 by trial and error, respectively. Since $\text{abs}(k_H) > \text{abs}(k_G)$, the priority of avoiding joint position limits is higher than that of avoiding joint velocity limits.

The proposed WGPM method with the performance criterion of avoiding joint velocity limits described as Eq. (36) is expressed as:

$$\dot{\theta} = E_c J_{E_c}^{\oplus, P_{E_c}} (\dot{x}_d + \kappa E_e) - P_{E_c}^{\oplus, P_{E_c}} (J_{B_k} T_r + k(G_n) \exp(0 E_c) \nabla G), \quad (38)$$

where the bandwidth for defining thresholds in normalization, λ , is set to 0.3.

The overview of the experimental setup is shown in Fig. 8, which mainly consists of the PC LabVIEW program, the motion control card and the redundant manipulator. These three parts communicate with each other to deliver the target and actual joint position by means of PCI and EtherCAT, and the traditional GPM method and the proposed WGPM method are embedded in the PC LabVIEW program to generate the target joint position. Moreover, the initial and terminal postures for manipulator in experiments are set as reference, and the terminal posture is also out of the manipulator's reachability, which is shown in Fig. 9. The trajectory is planned as a straight-line path of round-trip, i.e., $P_s \rightarrow P_f \rightarrow P_s$. Besides, the values of other parameters remain unchanged, as defined in the previous simulations.

Initial posture:

$$P_s = [0.4063, -0.238, 0.5969] \text{ [m]},$$

$$O_s = [-80.8661, 92.267, 79.244] \text{ [degree]}.$$

Terminal posture:

$$P_f = [0.5917, -0.2083, 0.104] \text{ [m]}$$

$$O_f = [-92.1895, 125.3982, 43.4023] \text{ [degree]}.$$

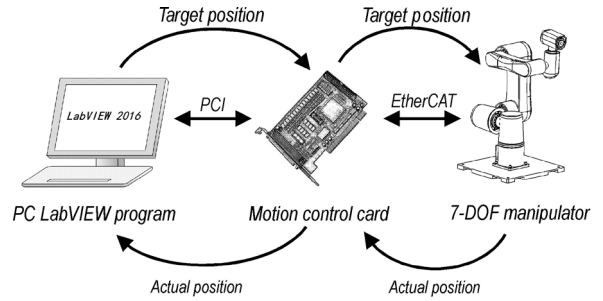


Fig. 8. Experimental setup

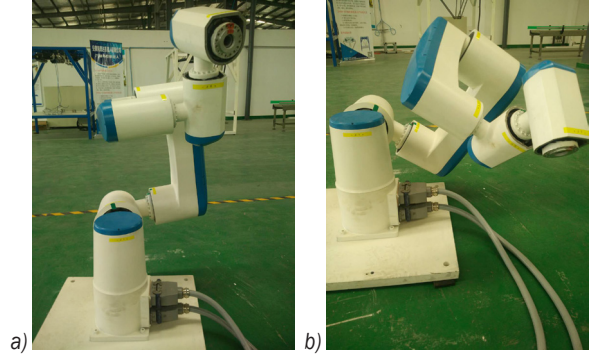


Fig. 9. Initial posture and terminal posture of the manipulator as reference; a) initial posture, and b) terminal posture

Fig. 10 illustrates the experimental results of the conventional GPM method. Seen from Fig. 10a, the second joint is approaching its position limit at $t=1.932$ s that leads to a singularity and motion deviation inevitably depicted in Figs. 10e and f, respectively. Since the influence of performance criterion of avoiding joint position limits defined in Eq. (11) is projected onto the null space shown in Fig. 10c, the second joint position limit is not violated with the smallest projected velocity by virtue of the advantage of redundancy.

However, it is noted that when tracking the large joint command velocities, extreme vibration chatter occurs at $t=1.428$ s shown in Fig. 10b. Eq. (37) defines a behaviour composed of main task and subtasks where the priority of avoidance of joint position limits is higher than that of avoidance of joint velocity limits but lower than the main task. Therefore, the projected velocities for avoiding joint velocity limits, depicted in Fig. 10d, are smaller than those for avoiding joint position limits even if the criterion of avoiding joint velocity limits is activated. Hence, the regulation between the main task and avoidances of joint position limits and joint velocity limits by the conventional GPM method failed.

The experimental results of the proposed WGPM method are summarized as shown in Fig.

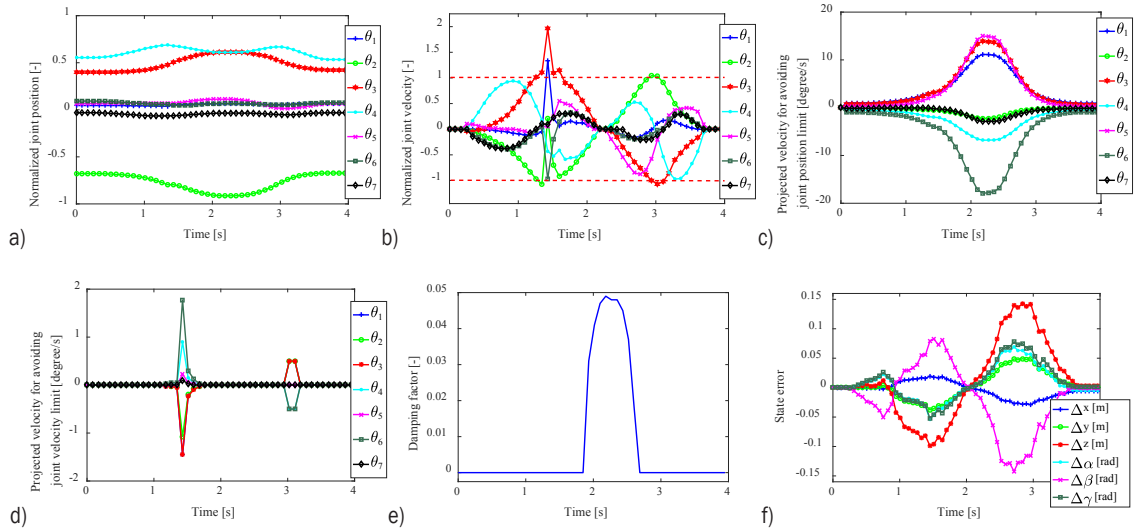


Fig. 10. Experiment results of the conventional GPM method with avoiding joint position limits and joint velocity limits; a) normalized joint position, b) normalized joint velocity, c) projected velocity produced from the performance criterion of avoiding joint position limits, d) projected velocity produced from the performance criterion of avoiding joint velocity limits, e) damping factor, and f) state error including position errors and orientation errors

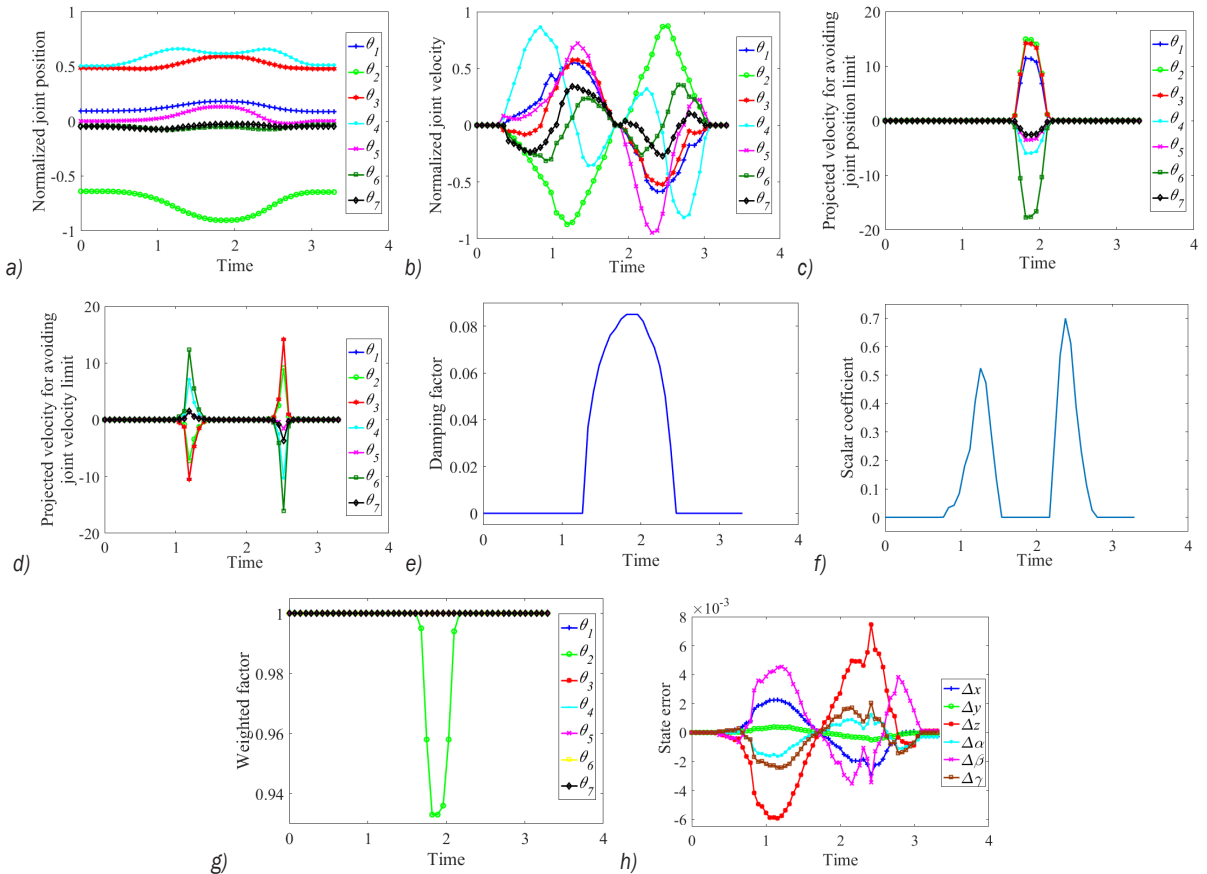


Fig. 11. Experiment results of the proposed WGPM method with avoiding joint position limits and joint velocity limits; a) normalized joint position, b) normalized joint velocity, c) projected velocity produced from the performance criterion of avoiding joint position limits, d) projected velocity produced from the performance criterion of avoiding joint velocity limits, e) damping factor, f) scalar coefficient of avoiding joint velocity limits, g) weighted factor from clamping matrix, and h) state error including position errors and orientation errors

11. Similarly, from Fig. 11a, the second joint is also close to its limit at $t=1.89$ s, and the corresponding weighted factor decreases to 0.933 in Fig. 11g according to the clamping weighted matrix operator with the appearance of singular configurations of the manipulator during $t=1.33$ s to 2.38 s. Remarkably, in the singular time shown in Fig. 11e, because the clamping matrix is not equal to an identity matrix, the repulsive potential field is activated to suppress the second joint velocity and repel it from its position limit effectively with a large opposite projected velocity, which passes through the weighted null space depicted in Fig. 11c. More significantly, however, from Figs. 10c and 11c, due to the different constructions of projected velocities for avoiding joint position limits between WGPM and GPM, the direction of the second joint projected velocity in WGPM is opposite to that in GPM.

From Fig. 11f, adopting the proposed continuous scalar coefficient theory, the coefficient for performance criterion of avoiding joint velocity limits is continuously documented dependent on the real-time joint velocities. Therefore, the projected velocities for avoiding joint velocity limits, shown in Fig. 11d, exist accompanied by the variation of the scalar coefficient and effectively restrain the joint velocity into a reasonable limit so as to protect and maintain the continuity of joint velocity. As such, the scheme to avoid joint velocity limits can play a positive effect on limiting joint velocities expressed as the normalizations depicted in Fig. 11b without any vibrations. Specifically, the scalar coefficient for avoiding joint velocity limits is automatically adjusted in WGPM while it is assigned a small constant value in GPM. Therefore, in Fig. 11d, two strong groups of projected velocities exist to avoid the second, the fourth and the fifth joint velocity violating their limits in the WGPM control while only an effective group, as shown in Fig. 10d, is produced from the conventional GPM control to constrain the first, the second, the third, and the sixth joint velocities.

The motion accuracies of the manipulator in experiments based on the traditional GPM method and the proposed WGPM method are demonstrated in Table 3. Obviously, the WGPM method has, compared to the GPM method, a potential advantage to enhance the kinematic performance of redundant manipulator that reduces errors by 6.27 %, 24.08 % and 45.33 % in position and by 44.81 %, 20.96 %, 12.04 % in orientation, respectively. Furthermore, as discussed previously, WGPM optimizes joint velocities in accordance with the clamping weighted matrix for avoiding joint position limits and the continuous scalar

coefficient for avoiding joint velocity limits while GPM does that all the time. Therefore, the proposed WGPM method could save time, i.e., decreasing 16.29 % of the time the GPM method consumed in the experiment.

Table 3. The maximum experimental results of state errors

	GPM	WGPM	Percentage [%]
Max Δx [m]	-0.0287	-0.0269	6.27
Max Δy [m]	0.049	0.0372	24.08
Max Δz [m]	0.1425	0.0779	45.33
Max $\Delta \alpha$ [rad]	0.0694	0.0383	44.81
Max $\Delta \beta$ [rad]	-0.1422	-0.1124	20.96
Max $\Delta \gamma$ [rad]	0.0781	0.0687	12.04
Running time [s]	3.948	3.305	16.29

Consequently, the main task with continuous joint positions and joint velocities is completed by means of the proposed WGPM method in which joint motion is subject to different performance criteria sufficiently, while the traditional GPM method is invalid.

4 CONCLUSIONS

The simulations and experiments in the paper are conducted to prove the validation and efficiency of the proposed WGPM method with multiple performance criteria. The results are concluded as follows:

1. Tracking the singular trajectory in simulations, the fourth joint and the seventh joint are successfully driven from joint position limits owing to exploitations of the proposed WGPM method, while they are arrested at limits using the WLN method that cannot repel them from limits. However, both methods violate joint velocity limits without taking into consideration the corresponding performance criterion.
2. The joint position limits and joint velocity limits are added to the experiments. In terms of guaranteeing the joint position limits, GPM performs as well as WGPM. In contrast, the regulation of avoiding joint velocity limits works barely satisfactory by using GPM that leads to a vibration chatter due to the unreasonable arrangement of fixed weights for multiple criteria. Contrarily, the hierarchical WGPM control effectively regulates the joint velocities far away limits based on the continuous scalar coefficient.
3. By analyses and comparisons of the simulation and experimental results, the hierarchical task-level regulation between the main task and subtasks in the proposed WGPM method is the

primary factor influence on improving kinematic motion prevision and saving time compared to the traditional WLN and GPM methods.

The paper provides a novel resolution to the IK problems of a redundant manipulator with multiple constraints. Future work will focus on the kinematical control of a redundant dual-arm manipulator.

5 ACKNOWLEDGEMENTS

The work supported by the National Natural Science Foundation (Grant no. 51375230, and Grant no. 51706098), China, and the Scientific and Technological Project in Anhui Province (Grant no. 1501021023), China.

6 REFERENCES

- [1] Giorelli, M., Renda, F., Calisti, M., Arienti, A., Ferri, G., Laschi, C. (2015). Neural network and Jacobian method for solving the inverse statics of a cable-driven soft arm with nonconstant curvature. *IEEE Transactions on Robotics*, vol. 31, no. 4, p. 823-834, DOI:10.1109/TRO.2015.2428511.
- [2] Cheng, G., Xu, P., Yang, D.H., Li, H., Liu, H.G. (2013). Analysing kinematics of a novel 3CPS parallel manipulator based on Rodrigues parameters. *Strojniški vestnik - Journal of Mechanical Engineering*, vol. 59, no. 5, p. 291-300, DOI:10.5545/sv-jme.2012.727.
- [3] Jin, L., Zhang, Y., Li, S., Zhang, Y. (2016). Modified ZNN for time-varying quadratic programming with inherent tolerance to noises and its application to kinematic redundancy resolution of robot manipulators. *IEEE Transactions on Industrial Electronics*, vol. 63, no. 11, p. 6978-6988, DOI:10.1109/TIE.2016.2590379.
- [4] Jin, L., Li, S. (2016). Distributed task allocation of multiple robots: A control perspective. *IEEE Transactions on Systems, Man, and Cybernetics: Systems*, vol. 48, no. 5, p. 693-701, DOI:10.1109/TSMC.2016.2627579.
- [5] Colomé, A., Torras, C. (2015). Closed-loop inverse kinematics for redundant robots: comparative assessment and two enhancements. *IEEE/ASME Transactions on Mechatronics*, vol. 20, no. 2, p. 944-955, DOI:10.1109/TMECH.2014.2326304.
- [6] Hu, T., Wang, T., Li, J., Qian, W. (2017). Gradient projection of weighted Jacobian matrix method for inverse kinematics of a space robot with a controlled-floating base. *ASME Journal of Dynamic Systems, Measurement, and Control*, vol. 139, no. 5, p. 051013-1-051013-10, DOI:10.1115/1.4035398.
- [7] He, X., Kong, X., Chablat, D., Caro, S., Hao, G. (2014). Kinematic analysis of a single-loop reconfigurable 7R mechanism with multiple operation modes. *Robotica*, vol. 32, no. 7, p. 1171-1188, DOI:10.1017/S0263574713001197.
- [8] He, X., Kong, X., Hao, G., Ritchie, J. (2016). Design and analysis of a new 7R single-loop mechanism with 4R, 6R and 7R operation modes. Ding, X., Kong, X., Dai, J. (eds.), *Mechanisms and Machine Science: Advances in Reconfigurable Mechanisms and Robots II*. Springer, Berlin, vol. 36, p. 27-37, DOI:10.1007/978-3-319-23327-7_3.
- [9] Kapoor, C., Cetin, M., Tesar, D. (1998). Performance based redundancy resolution with multiple criteria. *ASME Design Engineering Technical Conference*, p. 1-6.
- [10] Lee, K.K., Buss, M. (2006). Redundancy resolution with multiple criteria. *IEEE/RSJ International Conference on Intelligent Robots and Systems*, p. 598-603, DOI:10.1109/IROS.2006.282538.
- [11] Chaumette, F., Marchand, E. (2001). A redundancy-based iterative approach for avoiding joint limits: application to visual servoing. *IEEE Transactions on Robotics and Automation*, vol. 17, no. 5, p. 719-730, DOI:10.1109/70.964671.
- [12] Lu, B., Guo, S., Han, L. (2016). A coefficient matrix GPM method to avoid joint limits for fault tolerant redundant manipulators. *35th Chinese Control Conference (CCC)*, p. 7076-7081, DOI:10.1109/ChiCC.2016.7554475.
- [13] Li, L., Gruver, W.A., Zhang, Q., Yang, Z. (2001). Kinematic control of redundant robots and the motion optimizability measure. *IEEE Transactions on Systems, Man, and Cybernetics - Part B: Cybernetics*, vol. 31, no. 1, p. 155-160, DOI:10.1109/3477.907575.
- [14] Miyata, S., Miyahara, S., Nenchev, D. (2017). Analytical formula for the pseudoinverse and its application for singular path tracking with a class of redundant robotic limbs. *Advanced Robotics*, vol. 31, no. 10, p. 509-518, DOI:10.1080/01691864.2017.1285721.
- [15] Nakamura, Y., Hanafusa, H. (1986). Inverse kinematic solutions with singularity robustness for robot manipulator control. *ASME Journal of Dynamic Systems, Measurement, and Control*, vol. 108, no. 3, p. 163-171, DOI:10.1115/1.3143764.
- [16] Jin, L., Li, S., La, H.M., Luo, X. (2017). Manipulability optimization of redundant manipulators using dynamic neural networks. *IEEE Transactions on Industrial Electronics*, vol. 64, no. 6, p. 4710-4720, DOI:10.1109/TIE.2017.2674624.
- [17] Lopez, J., Brenosa, J., Galiana, I., Ferre, M., Gimenez, A., Barrio, J. (2012). Mechanical design optimization for multi-finger haptic devices applied to virtual grasping manipulation. *Strojniški vestnik - Journal of Mechanical Engineering*, vol. 58, no. 7-8, p. 431-443, DOI:10.5545/sv-jme.2011.141.
- [18] Xiang, J., Zhong, C., Wei, W. (2010). General-weighted least-norm control for redundant manipulators. *IEEE Transactions on Robotics*, vol. 26, no. 4, p. 660-669, DOI:10.1109/TRO.2010.2050655.
- [19] Chen, Y.J., Ju, M.Y., Hwang, K.S. (2017). A virtual torque-based approach to kinematic control of redundant manipulators. *IEEE Transactions on Industrial Electronics*, vol. 64, no. 2, p. 1728-1736, DOI:10.1109/TIE.2016.2548439.
- [20] Huang, S., Xiang, J., Wei, W., Chen, M.Z.Q. (2018). On the virtual joints for kinematic control of redundant manipulators with multiple constraints. *IEEE Transactions on Control Systems Technology*, vol. 26, no. 1, p. 65-76, DOI:10.1109/TCST.2017.2650684.
- [21] Flacco, F., De Luca, A., Khatib, O. (2015). Control of redundant robots under hard joint constraints: saturation in the null space. *IEEE Transactions on Robotics*, vol. 31, no. 3, p. 637-654, DOI:10.1109/TRO.2015.2418582.